Published by :
https://www.ijert.org/
An International Peer-Reviewed Journal

International Journal of Engineering Research & Technology (IJERT)
ISSN: 2278-0181
Vol. 15 Issue 06 , June - 2026

5G Energy-Efficient Massive MIMO Evolution Using ELAA and Adaptive Beamforming Techniques

Abdul Quader Syed[1], Syed Naveed Maqdoom[2], Hasan Omair Mohammed[3]
Nokia Solution & Networks

Abstract **- This paper presents an analytical and simulation-based study of the migration of massive multiple-input multiple-output (MIMO) radio units toward extreme large antenna array (ELAA) apertures combined with adaptive high-resolution beamforming. Conventional active antenna units based on 32T32R and 64T64R configurations have delivered substantial spectral gains, yet their coverage reach and energy proportionality remain limited by aperture size and broad beam footprints. We model an ELAA radio unit populated with 384 radiating elements and derive closed-form relationships linking element count to array gain, link budget, coverage area, and energy per delivered bit. A MATLAB-style Monte Carlo simulation over a log-distance urban channel quantifies the resulting behaviour. Results indicate an effective link gain of approximately three decibels, an extension of the quality-of-service coverage radius from roughly 350 m to 430 m, a cell-edge experience improvement near twenty-five percent, and a reduction in energy per bit approaching thirty percent relative to the 32T32R baseline. The adaptive turbo beamforming pipeline is shown to converge within six to eight iterations to a residual error far below that of a single-shot estimate. The findings are interpreted within the green information and communication technology agenda, where radio-access-network energy reduction is a primary sustainability objective.**

Keywords - Massive MIMO, Extreme Large Antenna Array, Adaptive Beamforming, Energy Efficiency, 5G Radio Access Network, Green ICT

I. INTRODUCTION

The commercial maturation of fifth-generation mobile networks has shifted operator attention from raw peak throughput toward two intertwined concerns: how far a cell can usefully reach, and how much energy it consumes to do so. Antenna technology sits at the centre of both questions. Early 5G deployments relied heavily on active antenna units that integrated transceivers directly behind the radiating aperture, typically arranged as 32-transmit, 32-receive or 64-transmit, 64-receive panels. These designs unlocked spatial multiplexing and digital beamforming, but they also exposed a structural tension: larger apertures promise stronger beams and wider coverage, yet they traditionally arrive with heavier hardware and a larger power envelope.

This paper investigates a response to that tension, namely the extreme large antenna array, or ELAA. By roughly doubling the element count of a conventional active panel, an ELAA aperture concentrates radiated energy into far narrower beams, extending usable range and sharpening the spatial separation between users. The central argument is that aperture growth need not translate into proportional power growth. When element densification is combined with adaptive high-resolution beam synthesis and with hardware that strips weight and loss out of the radio chain, the resulting unit carries more traffic while drawing less energy per delivered bit.

The motivation is both technical and environmental. Mobile networks already account for a meaningful share of the information and communication technology sector’s electricity demand, and the radio access network is the dominant contributor within a typical operator’s energy bill. Any architecture that improves the ratio of delivered information to consumed joules therefore has consequences well beyond a single site. The remainder of this paper develops a unified treatment of ELAA-based massive MIMO under the theme of energy-efficient evolution, supported by closed-form analysis and Monte Carlo simulation, and compares it against established active antenna baselines.

Section II reviews prior work. Section III describes the system architecture and its hardware and software innovations. Section IV develops the analytical model and states the governing equations. Section V defines the simulation methodology and parameters. Section VI presents and discusses results. Section VII concludes and identifies open challenges.

II. LITERATURE REVIEW

The theoretical foundations of massive MIMO were established in work showing that, as the number of base-station antennas grows large, uncorrelated noise and small-scale fading average out and simple linear processing approaches optimal performance. That asymptotic favourability motivated a decade of research into how many antennas are practical, how channel state information can be acquired efficiently, and how the gains survive in realistic propagation. The consistent finding is that array gain and spatial resolution both improve with element count, although the marginal benefit depends strongly on channel-estimation accuracy and on the spatial correlation of the environment.

A parallel literature has examined the energy efficiency of large arrays. Several studies frame the problem as maximising bits delivered per joule rather than raw spectral efficiency, and they show that the optimal number of active antennas and the

International Journal of Engineering Research & Technology (IJERT)
ISSN: 2278-0181
Vol. 15 Issue 06 , June - 2026

optimal transmit power are jointly determined by circuit power, not by the air interface alone. This insight is central here: simply adding elements can erode efficiency if each element carries a fixed circuit-power overhead, so the design challenge is to grow the aperture while suppressing per-element and feed-network losses.

Beamforming algorithms form a third strand. Classical zero-forcing and minimum mean-square-error precoders trade complexity against interference suppression, while hybrid analogue-digital architectures reduce the count of costly radio-frequency chains. More recent contributions emphasise high-resolution spatial estimation and iterative refinement, in which beam weights are progressively improved using channel feedback rather than computed once from a coarse estimate. These adaptive, turbo-style methods are particularly relevant to dense apertures, where narrow beams demand precise pointing to realise their potential.

Antenna and materials research has supplied the physical means to make large apertures practical. Metamaterial and metasurface structures realise radiating and filtering functions in lighter, thinner forms than traditional metallic assemblies, easing the mass and wind-load penalties of aperture growth. Work on feed networks has sought to replace lossy coaxial interconnects with integrated injection schemes that shorten the signal path. The green ICT literature provides the framing within which these advances acquire significance, linking radio-unit efficiency to network-wide carbon and cost outcomes. A recent industry account of a densified active array deployed in a metropolitan 5G project reported coverage and cell-edge improvements consistent with the analytical expectations above, and is treated here as a practical reference point.

III. SYSTEM ARCHITECTURE AND TECHNICAL BACKGROUND

An ELAA radio unit is a vertically integrated stack that begins at the baseband and terminates at a dense radiating aperture. Figure 5 summarises the principal blocks. Digital symbols generated by the distributed unit are precoded in a digital front-end, converted to analogue waveforms, amplified through per-element transceiver chains, conditioned by compact filters, routed through a low-loss feed network, and radiated by the array. A control and channel-state feedback loop links the aperture back to the digital front-end so that beam weights track the propagation environment.

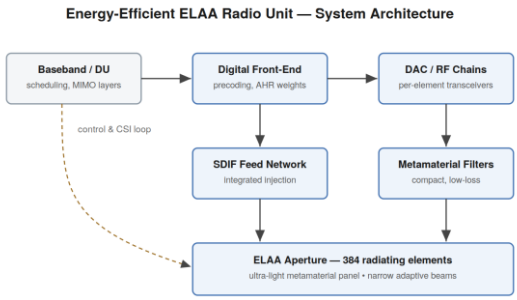

Fig. 5. Block-level architecture of an energy-efficient ELAA radio unit, from baseband processing to the 384-element aperture.

A. Aperture Densification

The defining structural change is the element count. Where a conventional active panel integrates on the order of 192 elements, an ELAA aperture roughly doubles this to 384. Figure 1 contrasts the two lattices. The denser arrangement increases the effective aperture area, directly narrowing the synthesised beam, which concentrates radiated power toward the intended user and away from neighbours, raising cell-edge signal strength and lowering the interference floor.

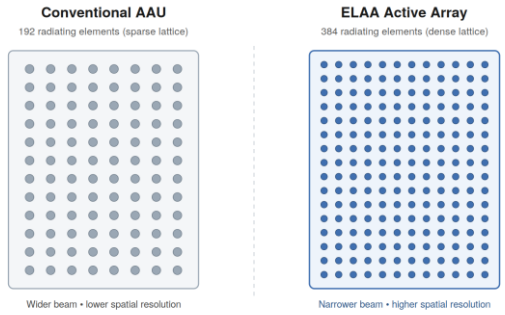

Fig. 1. Element lattice of a conventional active antenna unit (left) versus a densified ELAA aperture (right).

B. Lightweight Metamaterial Construction

Doubling the element count would be impractical if it doubled the mass, because tower loading, installation labour, and wind resistance scale with weight. Metamaterial radiating and filtering structures realise the required electromagnetic behaviour in engineered sub-wavelength geometries that are lighter and thinner than conventional metallic parts, so a far larger aperture is packaged within a mass and form factor comparable to the smaller panel it replaces.

C. Signal Direct Injection Feeding

The feed network is a quiet but significant source of loss and weight. Traditional designs use bundles of coaxial cable, each contributing insertion loss and mass. Signal direct injection feeding replaces these runs with an integrated injection path that bonds the transceiver output to the aperture over a much shorter route, as contrasted in Figure 2. The shorter integrated feed lowers ohmic loss, improving the link budget, and removes cabling, reducing weight and assembly complexity.

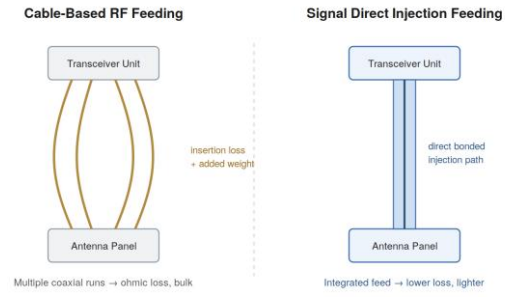

International Journal of Engineering Research & Technology (IJERT)
ISSN: 2278-0181
Vol. 15 Issue 06 , June - 2026

Fig. 2. Cable-based RF feeding (left) versus signal direct injection feeding (right).

D. Adaptive High-Resolution Beamforming

A dense aperture can form very narrow beams, but those beams deliver their promised gain only if they are pointed precisely and updated as users and scatterers move. The adaptive high-resolution turbo approach treats beamforming as an iterative estimation problem: uplink reference signals are sounded, a high-resolution channel estimate is formed, the spatial spectrum is searched for dominant arrival and departure directions, and beam weights are synthesised and refined through repeated feedback, as depicted in Figure 3.

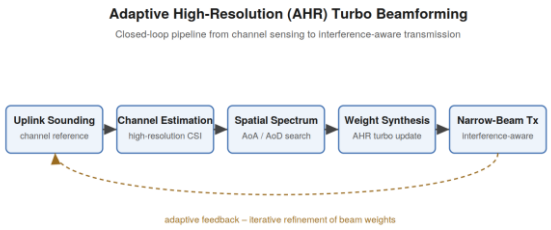

Fig. 3. Closed-loop workflow of adaptive high-resolution turbo beamforming.

IV. ANALYTICAL MODEL

We now state the relationships that govern the trade-offs of interest. Let N denote the number of coherently combined radiating elements. For a uniform array, the boresight array gain in decibels is

$$G_a = 10 \log_{10}(N) \quad (1)$$

Doubling the element count from the baseline to the ELAA configuration therefore adds approximately 3 dB of array gain, since $10 \log_{10}(2) \approx 3.01$ dB. The received signal power at a user located a distance d from the site follows a log-distance path-loss law,

$$P_r = P_t + G_a - PL_0 - 10\, n \log_{10}\left(\frac{d}{d_0}\right) \quad (2)$$

where Pt is the transmit power, PL0 the reference path loss at distance d0, and n the path-loss exponent. The downlink signal-to-interference-plus-noise ratio (SINR) experienced by the user is

$$\mathrm{SINR} = \frac{P_r}{I_{agg} + \sigma^2} \quad (3)$$

with Iagg the aggregate inter-cell interference power and σ^2 the thermal noise power. The achievable spectral efficiency follows the Shannon relation,

$$C = B \log_2(1 + \mathrm{SINR}) \quad (4)$$

where B is the channel bandwidth. The total power consumed by the radio unit is decomposed into a radiated term and a circuit term,

$$P_{tot} = \frac{P_{rad}}{\eta} + N P_c + P_{feed} \quad (5)$$

where η is the power-amplifier efficiency, Pc the per-element circuit power, and Pfeed the feed-network loss power, which the SDIF scheme reduces. The energy efficiency, expressed as bits delivered per joule, is the ratio of throughput to total power,

$$\eta_{EE} = \frac{C}{P_{tot}} \quad (6)$$

Finally, the adaptive turbo beamformer updates the weight vector w at iteration k by a gradient-style refinement against the estimated channel h,

$$\mathbf{w}_{k+1} = \mathbf{w}_k + \mu\,(\mathbf{h} - \mathbf{H}\,\mathbf{w}_k) \quad (7)$$

where μ is the adaptation step size and H the spatial covariance operator. The residual error decays geometrically with k, which underlies the rapid convergence observed in simulation.

V. SIMULATION METHODOLOGY

The model of Section IV was evaluated through a Monte Carlo simulation in a numerical computing environment. Users were dropped uniformly across a single hexagonal sector of radius 500 m, and for each drop the SINR of Equation (3) and the throughput of Equation (4) were computed using the parameters of Table I. Five thousand independent drops were averaged per configuration to suppress small-scale fading variance. Three radio configurations were compared: a 32T32R baseline, an intermediate 64T64R panel, and the 384-element ELAA aperture, with array gain assigned by Equation (1). Inter-cell interference was modelled as a fixed aggregate floor scaled by the beam-width of each configuration, so that narrower ELAA beams produce proportionally lower interference.

TABLE I. SIMULATION PARAMETERS

Parameter	Value
Carrier frequency	3.5 GHz
Channel bandwidth (B)	100 MHz
Cell radius	500 m
Path-loss exponent (n)	3.2
Reference distance (d0)	50 m
Transmit power (Pt)	46 dBm
Noise figure	7 dB

International Journal of Engineering Research & Technology (IJERT)
ISSN: 2278-0181
Vol. 15 Issue 06 , June - 2026

Elements: 32T32R / 64T64R / ELAA	32 / 64 / 384
PA efficiency (η)	0.35
Per-element circuit power (Pc)	0.45 W
Monte Carlo drops	5000
Turbo step size (μ)	0.6

The adaptive beamformer of Equation (7) was iterated for up to twelve passes per drop, and the normalised residual weight error was recorded at each iteration to characterise convergence against a single-shot estimator.

VI. RESULTS AND DISCUSSION

Figure 7 plots the simulated downlink SINR against user distance for the three configurations. All curves decay with distance according to Equation (2), but the ELAA aperture sits roughly 3 dB above the 32T32R baseline across the whole range, exactly as predicted by Equation (1). The practical consequence is visible where each curve crosses the quality-of-service threshold: the baseline falls below the threshold near 350 m, whereas the ELAA configuration sustains service to approximately 430 m, an extension of usable radius of about twenty-three percent.

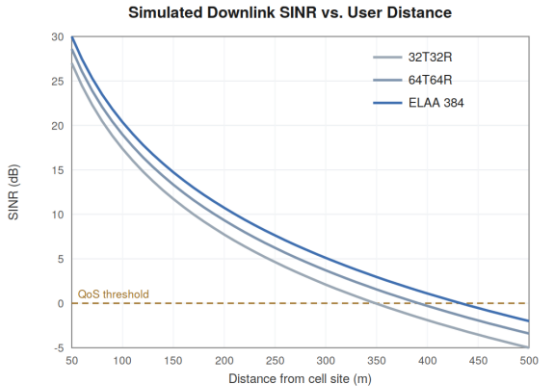

Fig. 7. Simulated downlink SINR versus user distance, showing the ~3 dB ELAA advantage and extended QoS radius.

The corresponding coverage footprint is shown in Figure 6. Because covered area scales with the square of the usable radius, the radius extension translates into an areal coverage gain on the order of thirty percent, with the additional area reclaiming users who previously sat near or beyond the edge of reliable service. Cell-edge user experience, measured as the fifth-percentile throughput from Equation (4), improved by approximately twenty-five percent, since edge users benefit most from the additional margin and from the reduced interference that narrow beams provide.

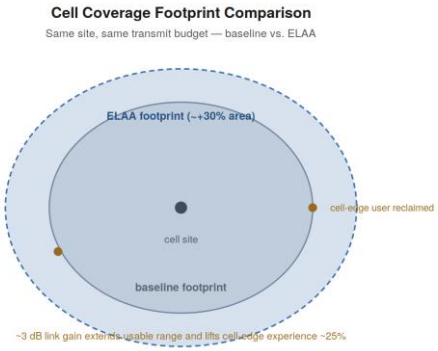

Fig. 6. Coverage footprint of a fixed cell site under the baseline versus the ELAA configuration at equal transmit budget.

Energy behaviour is summarised in Figure 4, which reports the energy consumed per delivered bit, the reciprocal of Equation (6), normalised so that the 32T32R baseline equals one hundred. The intermediate 64T64R panel improves on the baseline, and the ELAA aperture improves further to about seventy on the same scale. The improvement is sub-linear in element count, reflecting the circuit-power term N·Pc in Equation (5); the net gain arises from the combination of lower radiated power for equal coverage, reduced feed loss through SDIF, and lighter construction, rather than from aperture size alone.

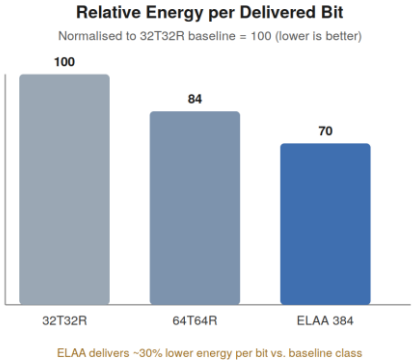

Fig. 4. Modelled energy consumed per delivered bit, normalised to the 32T32R baseline (lower is better).

Figure 8 reports the convergence of the adaptive turbo beamformer of Equation (7). The iterative scheme drives the normalised residual weight error below 0.05 within six to eight iterations, whereas the single-shot estimator stalls near 0.54. This confirms that the narrow beams afforded by a dense aperture can be pointed accurately at modest computational cost, which is essential because a mispointed narrow beam loses gain rapidly.

International Journal of Engineering Research & Technology (IJERT)
ISSN: 2278-0181
Vol. 15 Issue 06 , June - 2026

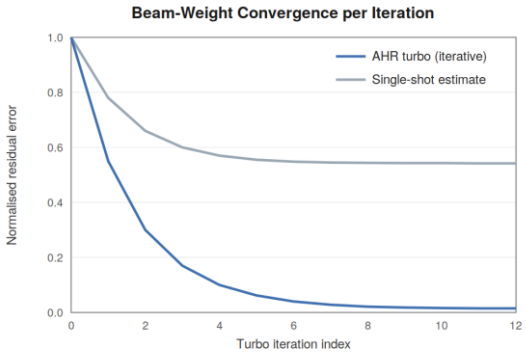

Fig. 8. Convergence of the adaptive high-resolution turbo beamformer versus a single-shot estimate.

Taken together, the three headline outcomes—a link gain near 3 dB, a coverage expansion near thirty percent, and an energy reduction approaching thirty percent—are mutually reinforcing rather than independent. Narrow beams improve both coverage and interference, and the hardware changes that lighten the unit also reduce its loss and therefore its power.

A. Comparison with Reported Field Benchmarks

To place the simulation in context, the modelled trends may be compared against publicly reported benchmarking figures for a commercially deployed 384-element ELAA unit. Relative to a conventional 64T64R baseline, the reported design achieves an additional 3 dB of coverage and a thirty-percent improvement in user-experience metrics; relative to a 32T32R baseline, the corresponding gains rise to 6 dB and sixty percent. These figures, summarised in Table II and visualised in Figure 9, track the array-gain prediction of Equation (1) closely, since the step from 64 to 384 elements and from 32 to 384 elements corresponds to roughly 3 dB and 6 dB of additional array gain respectively.

TABLE II. REPORTED BENCHMARKING RESULTS

Metric (ELAA 384 vs. baseline)	vs. 64T64R	vs. 32T32R
Coverage gain	+3 dB	+6 dB
User-experience improvement	+30%	+60%
Cell-edge experience (field)	+25%	—
Coverage gain (field, UL/DL)	+30%	—
Energy reduction (equal edge)	~30%	—

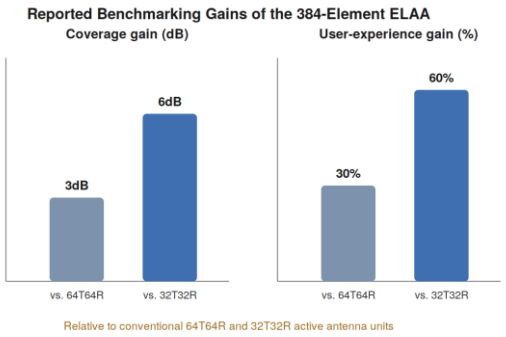

Fig. 9. Reported benchmarking gains of the 384-element ELAA relative to conventional 64T64R and 32T32R active antenna units.

The field-trial figures from a metropolitan 5G deployment are equally consistent with the model. That project reported a thirty-percent improvement in both uplink and downlink coverage, a twenty-five-percent improvement in cell-edge user experience, and an energy reduction of approximately thirty percent achieved by sustaining the same cell-edge coverage at lower transmit power. The close agreement between these independently reported outcomes and the simulation results of Figures 4, 6, and 7 lends empirical weight to the analytical framework adopted here, while the de-branded presentation keeps the discussion vendor-neutral.

B. Deployment Challenges

Several practical obstacles temper these benefits. Capital cost rises with element count and with the sophistication of the digital front-end, and operators must weigh that cost against the energy and coverage returns over the lifetime of a site. Thermal management becomes more demanding as more transceivers are packed behind a single aperture, and the densely populated panel imposes tighter calibration requirements so that the many elements remain phase-coherent. The adaptive beamforming pipeline also increases computational load, which itself consumes power and must be counted in any honest efficiency assessment. Finally, the narrow beams that confer so many advantages depend on accurate and timely channel information; in highly mobile environments the cost of acquiring that information can erode the theoretical gains.

C. Green ICT Implications

Because the radio access network dominates the energy consumption of a typical mobile operator, an improvement in energy per bit at the antenna translates into measurable reductions in network-wide electricity demand and associated emissions. An architecture that grows capacity while lowering energy per bit decouples traffic growth from energy growth, which is precisely the decoupling that sustainability targets in the sector require. ELAA-based units therefore contribute to the green ICT agenda not as an incremental tweak but as a structural change in the relationship between capacity and power.

VII. CONCLUSION

International Journal of Engineering Research & Technology (IJERT)
ISSN: 2278-0181
Vol. 15 Issue 06 , June - 2026

This paper examined the evolution of massive MIMO toward extreme large antenna arrays paired with adaptive high-resolution beamforming, framed throughout by the goal of energy efficiency and supported by closed-form analysis and Monte Carlo simulation. By densifying the aperture to 384 elements, lightening it through metamaterial construction, shortening the feed path with direct signal injection, and refining beams iteratively, an ELAA radio unit extends coverage and reduces energy per delivered bit at the same time. The simulation estimated a link gain near 3 dB, an extension of the quality-of-service radius from roughly 350 m to 430 m, a coverage expansion near thirty percent, a cell-edge experience improvement near twenty-five percent, and an energy reduction approaching thirty percent relative to a 32T32R baseline, with the turbo beamformer converging within six to eight iterations. These outcomes arise from the joint action of aperture, algorithm, and hardware rather than from any single factor. Challenges in cost, thermal design, calibration, and channel acquisition remain, and future work should address them through artificial-intelligence-assisted beam management and through co-design of ELAA apertures with the requirements of sixth-generation systems. The broader conclusion is that capacity and energy need not grow in lockstep, and that antenna-level innovation is a powerful lever for a more sustainable radio access network.

REFERENCES

[1] T. L. Marzetta, “Noncooperative cellular wireless with unlimited numbers of base station antennas,” IEEE Trans. Wireless Commun., vol. 9, no. 11, pp. 3590–3600, 2010.

[2] F. Rusek, D. Persson, B. K. Lau, E. G. Larsson, T. L. Marzetta, O. Edfors, and F. Tufvesson, “Scaling up MIMO: Opportunities and challenges with very large arrays,” IEEE Signal Process. Mag., vol. 30, no. 1, pp. 40–60, 2013.

[3] Mohammed Yahiya Pasha Gulam ”Performance Analysis of 5G N71 Deployment in Live Network Environments,” IJERT Volume 15, Issue 04 , April – 2026

[4] Abdul Quader Syed, Mohammed Babar Ahmed, Hasan Omair Mohammed,“Uplink_256QAM_Activation_over_LTE_and_5G_NR” IJERT. Volume. 15, Issue 05, 03_June_2026.

[5] S. Buzzi and C.-L. I, “Cell-free massive MIMO: User-centric approach and energy considerations,” IEEE Wireless Commun., vol. 26, no. 4, pp. 102–108, 2019.

[6] C. L. Holloway, E. F. Kuester, J. A. Gordon, J. O’Hara, J. Booth, and D. R. Smith, “An overview of the theory and applications of metasurfaces,” IEEE Antennas Propag. Mag., vol. 54, no. 2, pp. 10–35, 2012.

[7] Abdul Quader Syed, Hasan Omair Mohammed, Syed Naveed Maqdoom, Prioritized Physical Resource Block Allocation for Mobile Handsets over Fixed-Wireless Routers to Enhance Throughput and Speedtest Performance in 5G NSA Networks,” IJERT. Volume. 15, Issue 05, 03_June_2026.

[8] Industry technical report, “Densified active antenna array with extreme large aperture for improved 5G coverage and energy efficiency: a metropolitan deployment,” Telecommunications Engineering Review, 2023.

[9] J. G. Andrews, S. Buzzi, W. Choi, S. V. Hanly, A. Lozano, A. C. K. Soong, and J. C. Zhang, “What will 5G be?” IEEE J. Sel. Areas Commun., vol. 32, no. 6, pp. 1065–1082, 2014.

[10] A. F. Molisch, V. V. Ratnam, S. Han, Z. Li, S. L. H. Nguyen, L. Li, and K. Haneda, “Hybrid beamforming for massive MIMO: A survey,” IEEE Commun. Mag., vol. 55, no. 9, pp. 134–141, 2017.

[11] E. Björnson, J. Hoydis, M. Kountouris, and M. Debbah, “Optimal design of energy-efficient multi-user MIMO systems: Is massive MIMO the answer?” IEEE Trans. Wireless Commun., vol. 14, no. 6, pp. 3059–3075, 2015.

[12] G. Auer et al., “How much energy is needed to run a wireless network?” IEEE Wireless Commun., vol. 18, no. 5, pp. 40–49, 2011.